crystals

MDPI

Article

2-Azidoimidazolium Ions Captured by *N*-Heterocyclic Carbenes: Azole-Substituted Triazatrimethine Cyanines

Simone Haslinger [1], Gerhard Laus [1,*], Volker Kahlenberg [2], Klaus Wurst [1], Thomas Bechtold [3], Stefan Vergeiner [1] and Herwig Schottenberger [1]

1 Faculty of Chemistry and Pharmacy, University of Innsbruck, Innsbruck 6020, Austria; simone.haslinger@uibk.ac.at (S.H.); klaus.wurst@uibk.ac.at (K.W.); stefan.vergeiner@uibk.ac.at (S.V.); herwig.schottenberger@uibk.ac.at (H.S.)

2 Institute of Mineralogy and Petrography, University of Innsbruck, Innsbruck 6020, Austria; volker.kahlenberg@uibk.ac.at

3 Research Institute for Textile Chemistry and Textile Physics, University of Innsbruck, Dornbirn 6850, Austria; thomas.bechtold@uibk.ac.at

* Correspondence: gerhard.laus@uibk.ac.at; Tel.: +43-512-507-57080; Fax: +43-512-507-57099

Academic Editor: Helmut Cölfen

Received: 29 January 2016; Accepted: 17 February 2016; Published: 8 April 2016

Abstract: 1,3-Disubstituted 2-azidoimidazolium salts (substituents = methyl, methoxy; anion = PF_6) reacted with *N*-heterocyclic carbenes to yield yellow 2-(1-(azolinylidene)triazen-3-yl)-1,3-R_2-imidazolium salts (azole = 1,3-dimethylimidazole, 1,3-dimethoxyimidazole, 4-dimethylamino-1-methyl-1,2,4-triazole; R = methyl, methoxy; anion = PF_6). Crystal structures of three cationic triazenes were determined. Numerous interionic C–H···F contacts were observed. Solvatochromism of the triazenes in polar solvents was investigated by UV-Vis spectroscopy, involving the dipolarity π^* and hydrogen-bond donor acidity α of the solvent. Cyclovoltammetry showed irreversible reduction of the cations to uncharged radicals. Thermoanalysis showed exothermal decomposition.

Keywords: azide; carbene; cyanine; cyclovoltammetry; imidazole; thermoanalysis; triazene; triazole; UV-Vis spectroscopy

1. Introduction

Previously, the 2-azido-1,3-dimethoxyimidazolium [1] and 2-azido-1,3-dimethylimidazolinium [2] ions were synthesized from the respective 2-bromo or 2-chloro compounds and sodium azide. This pathway is only viable when the halogen derivatives are readily available. A different approach to azidoazoles involves fragmentation of sulfonyltriazenes [3], which can be accessed by azidation of azole anions. In addition, triazene formation is accomplished by reaction of imidazolin-2-ylidenes with alkyl or aryl azides [4,5], and a series of triazene crystal structures of this type are known [4–11]. One crystal structure of a cationic triazatrimethine cyanine chromophore derived from benzimidazole has been reported [12]. Other related structures include metal complexes of neutral [13–15] and anionic 1,3-bis(tetrazol-5-yl)triazene ligands [16,17]. In this work, we intended to combine the azidation of a carbene with the fragmentation of a sulfonyltriazene.

2. Results and Discussion

Since the 2-azido-1,3-dimethylimidazolium ion is not yet described, we attempted to prepare it by azidation of the respective carbene using tosyl azide (Figure 1).

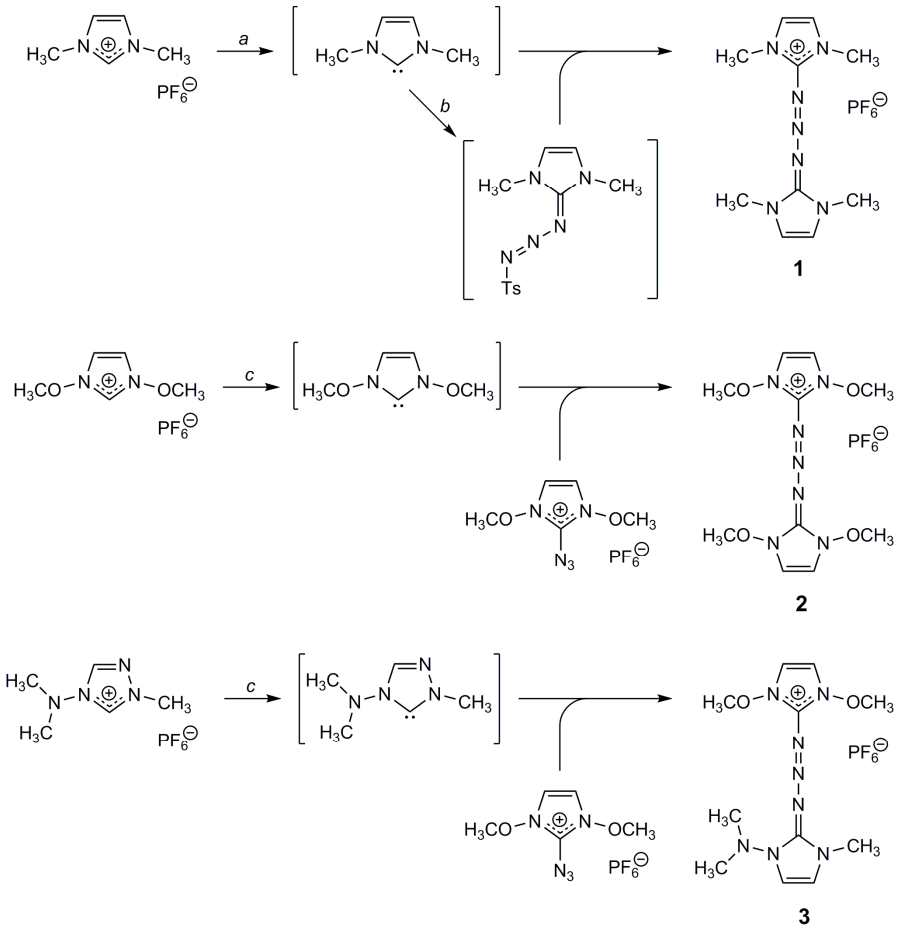

Figure 1. Synthesis of **1**–**3**. Reagents and conditions: *a*: $Li(Me_3Si)_2N$, THF; *b*: TsN_3; *c*: NaH, CH_3CN.

Surprisingly, it was found that the resulting tosyltriazene reacted with the intermediate carbene, yielding the disubstituted triazene **1**. The primary product mixture consisted of lithium toluenesulfinate and triazene and was easily separated. The desired 2-azidoimidazolium salt could not be isolated but will be attempted in further work. However, this result inspired us to prepare other triazenes, or triazatrimethine cyanines, from stable azidoazolium salts and *N*-heterocyclic carbenes. Thus, several methods to generate the carbenes were tested, and sodium hydride in acetonitrile was discovered to give agreeable results and allowed the synthesis of another symmetrically substituted triazene **2** and the unsymmetrically substituted triazene **3**.

The hexafluoridophosphate anions were chosen because they readily yield non-hygroscopic, crystalline solids. The role of fluorine, which exhibits the lowest polarizability and highest electronegativity of the halogens in crystal structures of organic compounds has been reviewed [18]. After some controversy, it has been concluded that short C–H$\cdots$F contacts between oppositely charged molecules are genuine interionic hydrogen bonds [19].

The crystal structures of the new cationic triazatrimethine cyanines **1**–**3** were determined and are discussed below.

2.1. Crystal Structures

The $C_{10}H_{16}N_7$ cation in triazene **1** contains 41.9% N and may be termed "nitrogen-rich". A crystal of **1** was refined as a two-component twin. Positional disorder of the fluorine atoms of PF_6 was observed, and a ratio of 3:2 was obtained by refinement as a free variable. In addition, the small crystal was non-merohedrally twinned by 180 degrees about the reciprocal axis 0 0 1.

The imidazole-substituted triazene system in **1** is heavily distorted. The angle between the planes of the two imidazole rings is 59.3°, the N5–N6 bond is rotated out of the plane of the first imidazole ring by 25.9°, and the N7–N6 bond is rotated out of the plane of the second imidazole ring by 32.4° (Figure 2a). Although the mesomeric cyanine molecule is symmetrically disubstituted, the bond lengths in the triazene bridge do not reflect this symmetry, presumably due to packing effects.

The heteroaromatic C2–H, C7–H and C8–H donate hydrogen bonds to F4, F3 and F1, whereas H atoms of one methyl group form contacts to F1 and F6 (Figure 2b).

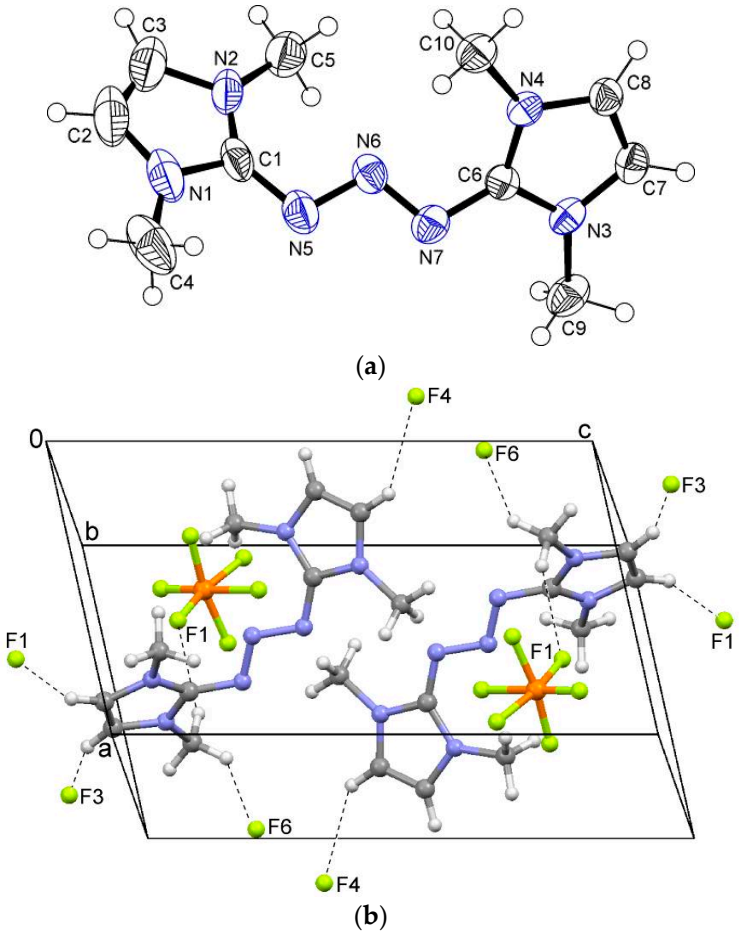

Figure 2. (**a**) Molecular structure of the cation; (**b**) interactions in the crystal structure of **1**.

Crystal data and structure refinement details are summarized in Table 1. Short contacts and interactions are listed in Table 2. Selected bond lengths, angles and torsions of the triazene bridge are compiled in Table 3.

The imidazole-substituted triazene system in **2** is far less distorted than in **1**. Thus, the angle between the planes of the two imidazole rings is 14.8°, the N5–N6 bond is twisted out of the plane of the adjacent imidazole ring by 7.6°, and the N7–N6 bond by 16.3°. The methoxy groups of both imidazole rings adopt *syn* conformations, although in opposite directions (Figure 3a).

Several C–H···F interactions involve the heteroaromatic C3–H, C7–H and C8–H, as well as the C9 methyl group. Additionally, C2–H···O3 and C4–H···O4 interactions are observed (Figure 3b).

The PF_6-groups in **2** and **3** were orientationally disordered among two positions. SADI commands were employed to restrain the corresponding P–F and F–F distances. For the refinement of the anisotropic displacement parameters, SIMU commands were used for atoms closer than 1.0 Å.

Table 1. Crystal data and structure refinement for **1**–**3**.

Compound	**1**	**2**	**3**
CCDC No.	1428586	1428587	1428588
Empirical formula	$C_{10}H_{16}N_7 \cdot F_6P$	$C_{10}H_{16}N_7O_4 \cdot F_6P$	$C_{10}H_{18}N_9O_2 \cdot F_6P$
Formula weight	379.27	443.27	441.3
Crystal system	Triclinic	Monoclinic	Monoclinic
Space group	$P\bar{1}$	$P2_1/c$	$P2_1$
a/Å	7.608 (1)	10.354 (1)	10.567 (1)
b/Å	8.386 (1)	13.153 (1)	6.573 (1)
c/Å	13.806 (1)	13.863 (1)	14.267 (2)
α/°	80.893 (2)	–	–
β/°	77.396 (2)	109.841 (8)	111.390 (11)
γ/°	70.006 (2)	–	–
Volume/Å^3	804.5 (1)	1775.8 (2)	922.6 (2)
Z	2	4	2
D_x/g·cm^{-3}	1.57	1.66	1.59
μ/mm^{-1}	0.24	0.25	0.24
F (000)	388	904	452
T/K	170 (2)	173 (2)	173 (2)
Crystal size/mm^3	0.18 × 0.15 × 0.03	0.40 × 0.28 × 0.08	0.38 × 0.32 × 0.28
θ_{max}/°	25.0	25.4	25.3
Index ranges	$-8 \leqslant h \leqslant 9$, $-9 \leqslant k \leqslant 9$, $0 \leqslant l \leqslant 16$	$-12 \leqslant h \leqslant 12$, $-15 \leqslant k \leqslant 15$, $-12 \leqslant l \leqslant 16$	$-12 \leqslant h \leqslant 10$, $-7 \leqslant k \leqslant 7$, $-15 \leqslant l \leqslant 17$
Reflections collected	3311	11235	5556
Independent reflections (R_{int})	3311	3251 (0.026)	3303 (0.023)
Observed reflections ($I > 2\sigma(I)$)	2651	2701	3215
Absorption correction	multi-scan	multi-scan	multi-scan
Restraints/parameters	0/278	162/312	157/313
Goodness-of-fit on F^2	1.04	1.04	1.10
R_1/wR_2 ($I > 2\sigma(I)$)	0.057/0.124	0.037/0.088	0.031/0.078
R_1/wR_2 (all data)	0.080/0.134	0.048/0.094	0.032/0.079
$\Delta\rho_{max}/\Delta\rho_{min}$/e·Å^{-3}	0.277/–0.426	0.44/–0.26	0.24/–0.19

The unsymmetrically disubstituted triazene system in **3** is the least distorted of the three compounds. The angle between the planes of the two heterocyclic rings is only 4.8°, the N5–N6 bond is rotated out of the imidazole plane by 10.5°, and the N7–N6 bond out of the triazole plane by 13.5° (Figure 4a). Again, the methoxy groups adopt *syn* conformation. In contrast to **1**, although the cyanine molecule is unsymmetrically disubstituted, the corresponding bond lengths in the triazene bridge are almost equal. A comparison of the bond lengths in the triazenes with accepted values [20] reveals the delocalized nature of the bonds in these systems. The N···N distances here are longer than trans N=N bonds (1.22 A), but shorter than typical planar N–N bonds (1.40 A). In addition, the C···N distances are longer than C=N bonds (1.28 A) but shorter than isolated C–N= bonds (1.43 A). The bonds in the triazenes compare favorably to aromatic N=N (1.30 A) and C=N (1.34 A) bonds.

Table 2. Interactions for **1**–**3** (Å, °).

Compound	Interaction	H···*A*	C···*A*	C–H···*A*	Symmetry Operation *A*
1	C8–H···F1	2.417	3.28 (1)	151.0	$x, y, 1 + z$
	$C9–H_C···F1$	2.417	3.18 (1)	134.5	$1 - x, 1 - y, 1 - z$
	C7–H···F3	2.422	3.26 (2)	146.4	$x, -1 + y, 1 + z$
	$C9–H_A···F6$	2.456	2.99 (1)	114.1	$-x, 1 - y, 1 - z$
	$C10–H_A···F5$	2.463	3.19 (1)	130.7	$1 - x, 2 - y, 1 - z$
	C2–H···F4	2.570	3.17 (1)	131.2	$1 + x, y, z$
2	C2–H···O3	2.295	3.128 (3)	146.0	$1 - x, 1/2 + y, 3/2 - z$
	$C7–H···F6_A$	2.281	3.21 (1)	167.3	$2 - x, -1/2 + y, 3/2 - z$
	$C8–H···F3_A$	2.384	3.24 (1)	149.8	$2 - x, -y, 1 - z$
	$C9–H_B···F1_A$	2.414	3.02 (1)	119.5	$x, 1/2 - y, 1/2 + z$
	$C3–H···F5_A$	2.460	3.30 (1)	147.6	$1 - x, 1 - y, 1 - z$
	$C4–H_C···O4$	2.575	3.355 (3)	136.6	$1 - x, -y, 1 - z$
3	$C3–H···F6_A$	2.512	3.34 (1)	145.3	$x, 1 + y, z$
	$C3–H···F3_A$	2.542	3.27 (1)	133.1	$x, 1 + y, z$
	$C7–H···F5_A$	2.339	3.18 (1)	147.2	$1 + x, -1 + y, z$
	$C9–H_B···F5_A$	2.446	3.42 (1)	173.7	$1 - x, -1/2 + y, - z$
	$C4–H_B···F1_A$	2.421	3.19 (1)	134.6	$1 - x, -1/2 + y, 1 - z$
	$C4–H_A···F3_A$	2.464	3.10 (1)	121.8	$1 - x, 1/2 + y, 1 - z$
	$C10–H_C···N5$	2.584	3.378 (4)	138.1	$x, -1 + y, z$
	$C5–H_B···N7$	2.555	3.480 (3)	157.5	$1 - x, 1/2 + y, -z$
	$C8–H_B···O1$	2.385	3.349 (2)	168.2	$2 - x, -1/2 + y, 1 - z$

Table 3. Selected bond lengths, angles and torsions of the triazene bridge for **1**–**3** (Å, °).

Compound	1	2	3
C1–N5	1.359 (7)	1.353 (3)	1.353 (3)
N5–N6	1.319 (4)	1.302 (2)	1.304 (3)
N6–N7	1.296 (5)	1.309 (3)	1.303 (3)
N7–C6	1.374 (4)	1.351 (2)	1.356 (3)
C1–N5–N6	110.3 (3)	113.3 (2)	114.5 (2)
N5–N6–N7	111.3 (3)	109.8 (2)	110.0 (2)
N6–N7–C6	110.0 (3)	112.9 (2)	113.0 (2)
C1–N5–N6–N7	173.9 (3)	177.7 (2)	177.1 (2)
N5–N6–N7–C6	175.0 (3)	179.9 (2)	178.2 (2)

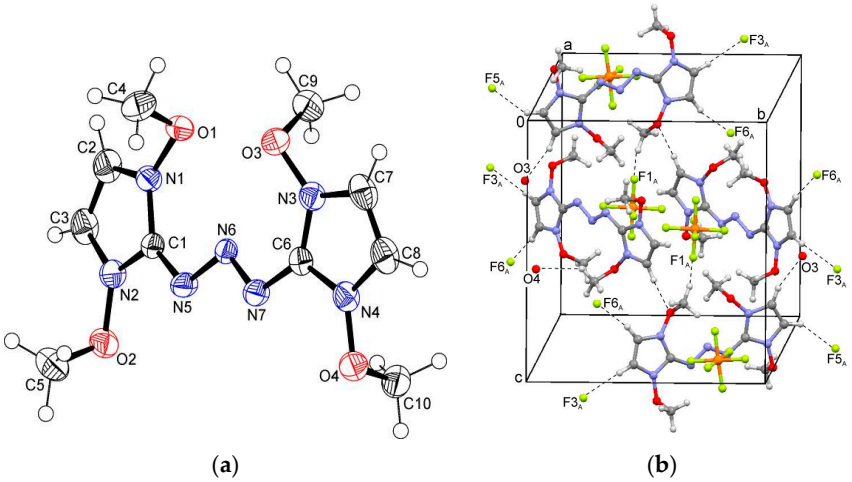

(**a**) (**b**)

Figure 3. (**a**) Molecular structure of the cation; (**b**) interactions in the crystal structure of **2**.

In the structure of **3**, the heteroaromatic C7–H of the triazole donates a hydrogen bond to F5, whereas the C3–H of the imidazole forms bifurcated hydrogen bonds to F3 and F6. Aliphatic hydrogen atoms form contacts to F1, F3 and F5, as well as to O1 and N7 (Figure 4b).

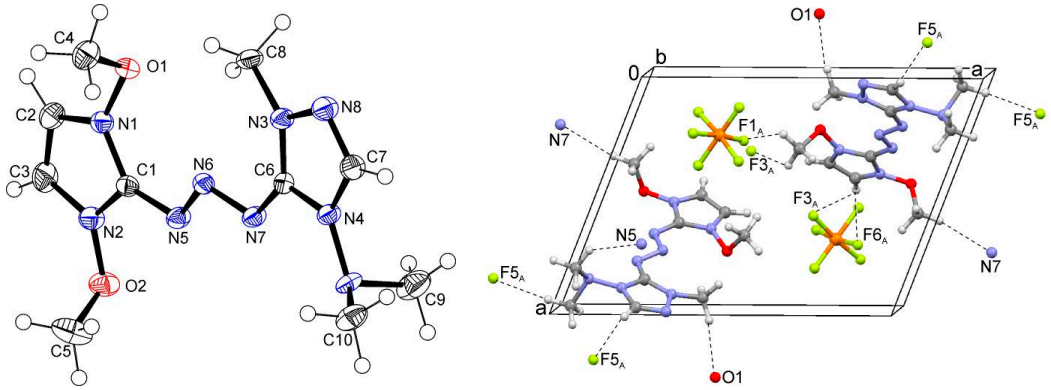

Figure 4. (**a**) Molecular structure of the cation; (**b**) interactions in the crystal structure of **3**.

2.2. UV-Vis Spectroscopy

Typically, donor–acceptor-substituted conjugated systems exhibit solvatochromism. The solvatochromism of such systems arises from the different stabilization of their electronic ground and excited state by differential solvation of these two states, according to their different molecular and electronic structure. Transition energies E_T were calculated from the wavelengths of the absorption maxima (Table 4) according to the equation $E_T/\mathrm{kJ\cdot mol^{-1}} = hcN/\lambda = 119625/(\lambda/\mathrm{nm})$. A linear solvation energy relationship was established by least-squares fitting the data to the solvatochromic equation involving the parameters π^* [21] and α [22] which represent the dipolarity/polarizability and hydrogen-bond donor capabilities of the solvent.The hydrogen-bond acceptor basicity β [23] did not significantly contribute to the relationship. The following equations were derived by multiple linear regression (Figure 5), which adequately describe the solvatochromic behavior of the triazenes.

$$\text{For } \mathbf{1}: \; E_T/\mathrm{kJ\cdot mol^{-1}} = 291.7 + 3.98\,\pi^* + 8.61\,\alpha \; (n = 7,\; R^2 = 0.992)$$

$$\text{For } \mathbf{2}: \; E_T/\mathrm{kJ\cdot mol^{-1}} = 313.2 - 9.21\,\pi^* - 5.08\,\alpha \; (n = 6,\; R^2 = 0.960)$$

$$\text{For } \mathbf{3}: \; E_T/\mathrm{kJ\cdot mol^{-1}} = 317.96 + 3.32\,\pi^* + 8.15\,\alpha \; (n = 6,\; R^2 = 0.960)$$

The triazenes **1** and **3** exhibited negative solvatochromism (shift of the absorption maximum to shorter wavelengths on changing the solvent from dichloromethane to water) whereas, amazingly, triazene **2** displayed positive solvatochromism. No correlation was found with less polar solvents.

Table 4. Solvent parameters and absorption maxima of the triazenes **1–3** in polar solvents.

Solvent	π^*	α	**1**	**2**	**3**
			λ_{max}/nm	λ_{max}/nm	λ_{max}/nm
H_2O	1.09	1.17	391.0	403.0	361.5
AcOH	0.64	1.12	393.0	396.0	362.8
MeOH	0.60	0.98	395.5	394.5	364.3
EtOH	0.54	0.86	397.5	393.7	367.5
2-PrOH	0.48	0.76	399.0	393.7	367.0
CH_2Cl_2	0.82	0.13	403.5	392.0	371.7
DMSO	1.00	0	405.0	–	–

The values in DMSO for **2** and **3** were not included in the calculation because a change of band shape rendered them not comparable. The π^* and α values were taken from the compilation of Marcus [24].

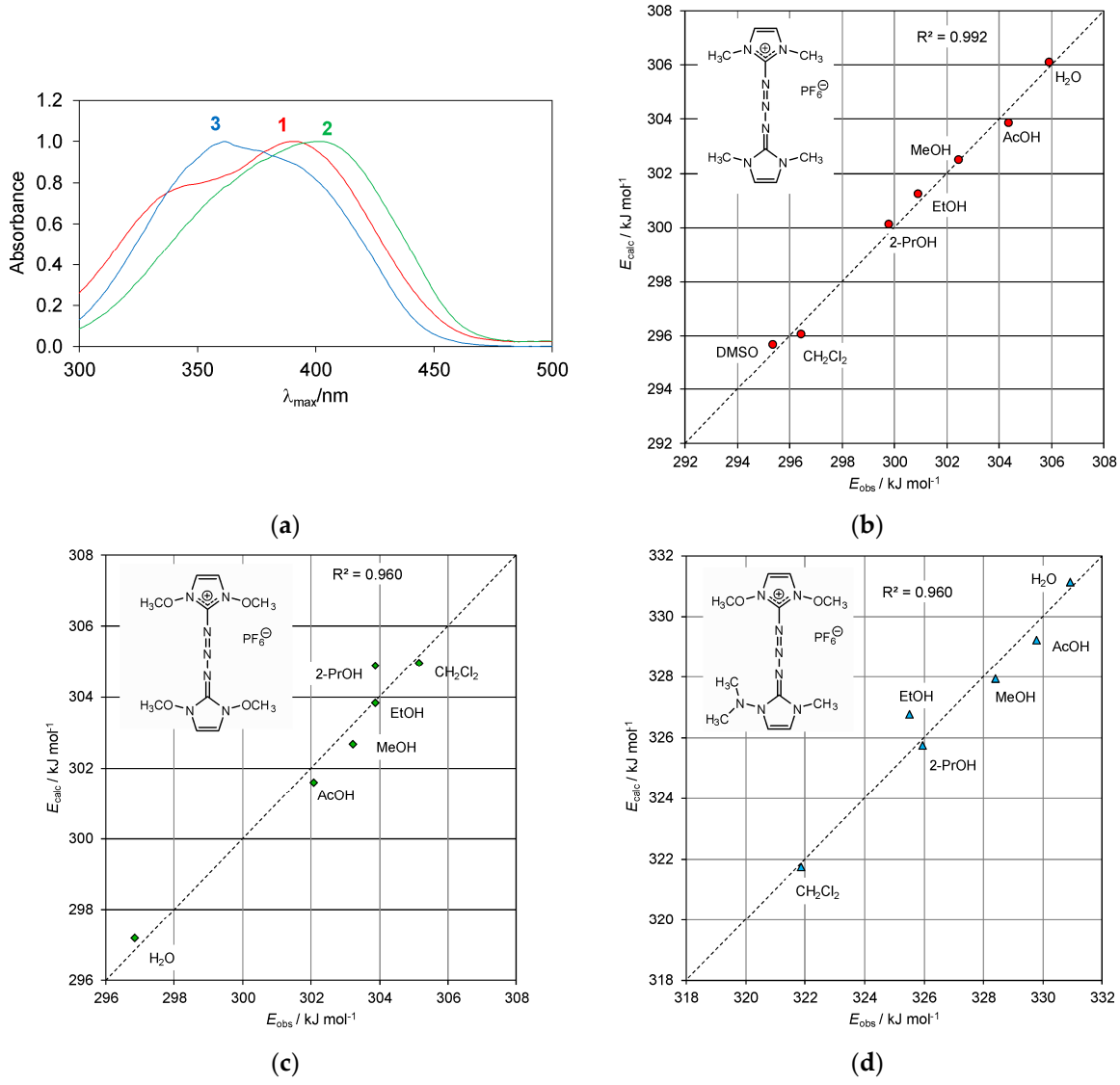

Figure 5. (**a**) Normalized UV-Vis spectra of triazenes **1**–**3** in H_2O. (**b**–**d**) correlation of observed *vs.* calculated transition energies of triazenes **1**–**3** in polar solvents.

2.3. Differential Scanning Calorimetry (DSC) and Thermogravimetric Analysis (TGA)

Thermoanalysis showed exothermal decomposition (maxima at 282 for **1**, 180 for **2** and 186 °C for **3**) with considerable mass loss (Figure 6).

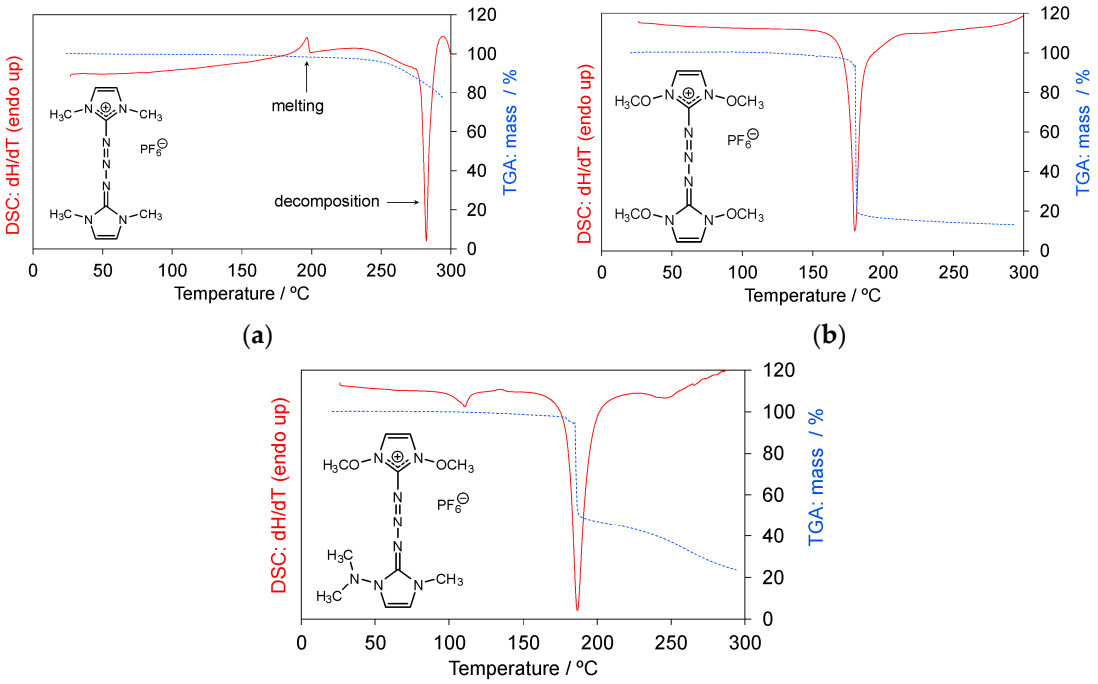

Figure 6. (**a**–**c**) DSC and TGA of the triazenes **1**–**3**.

2.4. Cyclic Voltammetry (CV)

The three electrophoric systems have in common that no reverse peaks were observed. Presumably, the first electrochemical process involved an irreversible reduction to an uncharged radical species. The resulting radical evidently was unstable on the electrochemical time scale and underwent subsequent decomposition. The cathodic peak current $(I_p)_c$ was approximately proportional to the square root of the scan rate, and the cathodic peak potential $(E_p)_c$ shifted to negative values with an increasing rate (Figure 7). The peak potential and peak current values found in the voltammetric measurements are summarized in Table 5.

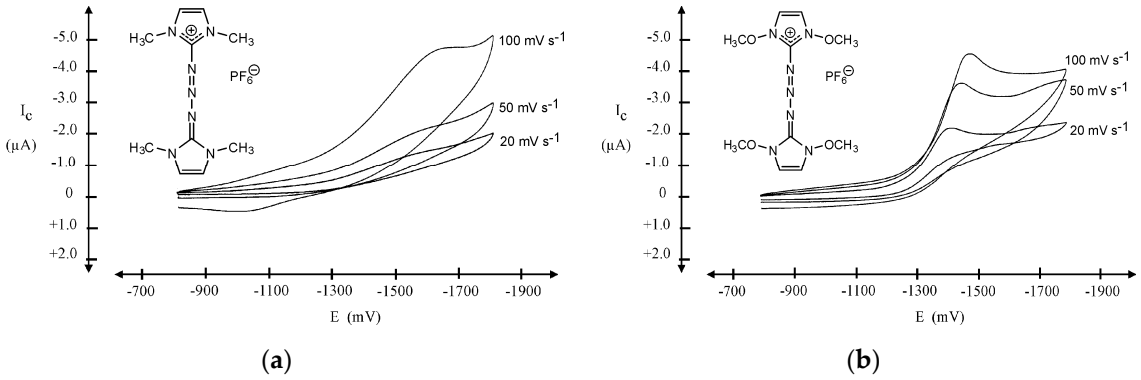

Figure 7. *Cont.*

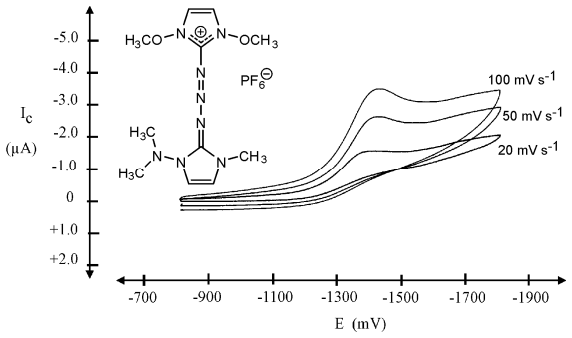

(**c**)

Figure 7. (**a**–**c**) Cyclic voltammograms of the triazenes **1**–**3**.

Table 5. Cathodic peak potential $(E_p)_c$ and cathodic peak current $(I_p)_c$ of the triazenes **1**–**3** in CH_3CN/0.1 M Bu_4PF_6 as function of scan rate (potential values *vs.* ferrocene couple).

Compound	Scan rate/mV·s^{-1}	$(E_p)_c$/mV	$(I_p)_c$/μA
1	20	n.d.	0.6
	50	n.d.	0.9
	100	−1470	2.4
2	20	−1410	1.8
	50	−1445	3.0
	100	−1475	3.8
3	20	−1390	1.2
	50	−1420	2.0
	100	−1430	2.7

3. Experimental Section

1,3-Dimethylimidazolium hexafluoridophosphate, 2-azido-1,3-dimethoxyimidazolium hexafluoridophosphate, 1,3-dimethoxyimidazolium hexafluoridophosphate, and 4-(dimethylamino)-1-methyl-1,2,4-triazolium hexafluoridophosphate were prepared as described previously [1,25,26]. All other chemicals were purchased from Sigma-Aldrich, St. Louis, MO, USA (European affiliate, Steinheim, Germany). NMR spectra were recorded with a Bruker Avance DPX 300 spectrometer (Billerica, MA, USA). IR spectra were obtained with a Nicolet 5700 FT spectrometer (Thermo Fisher Scientific Inc., Waltham, MA, USA) in ATR mode. UV-Vis spectra were recorded with a Perkin-Elmer Lambda XLS+ spectrometer (Waltham, MA, USA); mean values of at least three replicates were taken. High resolution mass spectra were measured with a Finnigan MAT 95 mass spectrometer (Waltham, MA, USA). DSC and TGA were recorded with Perkin-Elmer DSC 7 and TGA 7 instruments (Waltham, MA, USA) at a heating rate of 10 °C·min^{-1} under nitrogen.

Cyclic voltammetric (CV) experiments were performed in CH_3CN at room temperature under Ar atmosphere using an EG&G 264 A polarographic analyser/stripping voltammeter (Princeton Applied Research, Oak Ridge, TN, USA). All measurements were carried out employing a three-electrode configuration consisting of a Pt electrode (disk, 2 mm diameter) as a working electrode and an (Ag/0.01 M $AgNO_3$ in CH_3CN) electrode as the reference (EG&G Micro-Cell). A Pt wire in an electrode bridge tube filled with supporting electrolyte and separated from the sample by a porous frit served as the counter electrode. A solution of 0.1 M Bu_4PF_6 in CH_3CN served as the supporting electrolyte. Sample solutions were prepared by dissolving triazene (2.5 mg) in electrolyte (25 mL). A solution of ferrocene in electrolyte was used for calibration. All formal potentials are referenced to the ferrocene/ferrocenium redox couple.

Single crystal diffraction intensity data were recorded by φ and ω scans with a Bruker D8 Quest Photon 100 (Billerica, MA, USA) (compound **1**), or by ω scans with an Oxford Diffraction Gemini-R Ultra (Oxford Diffraction Ltd., Abingdon, Oxfordshire, UK) (compounds **2** and **3**) diffractometer using Mo*K*α radiation. The structures were solved by direct methods and refined by full-matrix least-squares techniques on F^2. Programs CELL_Now and TWINABS (Bruker) were used for cell search of twin components and absorption correction. CCDC 1428586–1428588 contain the supplementary crystallographic data for this paper. These data can be obtained free of charge via http://www.ccdc.cam.ac.uk/conts/retrieving.html.

*3.1. 1,3-Dimethyl-2-(1-(1,3-dimethylimidazolin-2-ylidene)triazen-3-yl)imidazolium Hexafluoridophosphate (**1**)*

A solution of lithium bis(trimethylsilyl)amide in THF (5.4 mL 1 M, 1.3 equiv) was added to a suspension of 1,3-dimethylimidazolium hexafluoridophosphate (1.0 g, 4.1 mmol) in THF (10 mL) at 0 °C. The resulting solution was stirred for 30 min at 0 °C, then tosyl azide (0.41 g, 0.5 equiv) in THF (1 mL) was added. The mixture was stirred for 4 h at room temperature, then cooled at 0 °C again. The orange precipitate was collected by filtration and partitioned between CH_2Cl_2 (15 mL) and H_2O (15 mL). The aqueous phase was extracted once more with CH_2Cl_2 (10 mL), and the combined organic phases were dried over $MgSO_4$ and taken to dryness under reduced pressure to yield the triazene **1** as an orange powder (0.25 g, 35%). Single crystals were obtained from H_2O/acetone. M.p. 201 °C (decomposition). ^{1}H NMR (DMSO-d_6, 300 MHz, δ): 3.68 (s, 12H), 7.39 (s, 4H) ppm. ^{13}C NMR (DMSO-d_6, 75 MHz, δ): 35.1 (4C), 119.8 (4C), 147.9 (2C) ppm. IR (neat): $\tilde{\nu}$ 3174 (w), 3143 (w), 1573 (w), 1520 (m), 1503 (m), 1343 (w), 1272 (m), 1222 (m), 1099 (m), 827 (s), 755 (m), 711 (m), 700 (m), 555 (s) cm^{-1}. HRMS (ES): m/z = 234.143 (calcd. 234.146 for $C_{10}H_{16}N_7$, $[M]^+$).

*3.2. 1,3-Dimethoxy-2-(1-(1,3-dimethoxyimidazolin-2-ylidene)triazen-3-yl)imidazolium Hexafluoridophosphate (**2**)*

1,3-Dimethoxyimidazolium hexafluoridophosphate (0.10 g, 0.0004 mol) and 2-azido-1,3-dimethoxyimidazolium hexafluoridophosphate (0.12 g, 0.0004 mol) were dissolved in CH_3CN (5 mL). The resulting solution was cooled to 0 °C, and NaH (0.015 g, 0.0004 mol) was slowly added. A yellow precipitate was formed instantaneously, and the mixture was stirred for another 3 h. Subsequently, the solvent was evaporated, and the yellow residue was recrystallized from H_2O/acetone leading to yellow plates. Yield: 0.04 g (25%). M.p. 165 °C (decomposition). ^{1}H NMR (DMSO-d_6, 300 MHz, δ): 4.08 (s, 12H), 7.98 (s, 4H) ppm. ^{13}C NMR (DMSO-d_6, 75 MHz, δ): 67.9 (4C), 113.5 (4C), 141.5 (2C) ppm. IR (neat): $\tilde{\nu}$ 3167 (w), 3147 (w), 1556 (m), 1500 (m), 1247 (m), 1159 (m), 1053 (m), 1044 (m), 946 (m), 824 (s), 677 (m), 554 (s) cm^{-1}. HRMS (ES): m/z = 298.124 (calcd. 298.126 for $C_{10}H_{16}N_7O_4$, $[M]^+$).

*3.3. 1,3-Dimethoxy-2-(1-(1-methyl-4-dimethylamino-1,2,4-triazolin-5-ylidene)triazen-3-yl)imidazolium Hexafluoridophosphate (**3**)*

4-(Dimethylamino)-1-methyltriazolium hexafluoridophosphate (0.31 g, 0.0011 mol) and 2-azido-1,3-dimethoxyimidazolium hexafluoridophosphate (0.36 g, 0.0011 mol) were dissolved in CH_3CN (5 mL). The resulting solution was cooled to 0 °C, and NaH (0.05 g, 0.0011 mol) was slowly added. A yellow precipitate was formed instantaneously, and the mixture was stirred for another hour. Subsequently, the solvent was evaporated, and the residue was washed with H_2O (3 × 2 mL) and acetone (2 × 2 mL) leading to a yellow powder. The crude product was recrystallized from H_2O/acetone yielding bright yellow needles. Yield: 0.22 g (43%). M.p. 172 °C (decomposition). ^{1}H NMR (DMSO-d_6, 300 MHz, δ): 2.95 (s, 6H), 3.91 (s, 3H), 4.10 (s, 6H), 8.03 (s, 2H), 9.25 (s, 1H) ppm. ^{13}C NMR (DMSO-d_6, 75 MHz, δ): 46.3 (2C), 68.0 (2C), 113.7 (2C), 139.7, 141.1, 151.8 ppm. ^{1}H NMR (acetone-d_6, 300 MHz, δ): 3.10 (s, 6H), 4.04 (s, 3H), 4.23 (s, 6H), 7.81 (s, 2H), 8.84 (s, 1H) ppm. ^{13}C NMR (acetone-d_6, 75 MHz, δ): 40.3, 46.7 (2C), 68.8 (2C), 114.6 (2C), 140.7 (2C), 154.0 ppm. IR (neat): $\tilde{\nu}$ 3167 (w), 3152 (w), 2923 (w), 2851 (w), 1546 (m), 1506 (m), 1453 (m), 1272 (m), 1242 (m), 1170 (m),

1160 (m), 1047 (m), 817 (s), 682 (m), 555 (s) cm^{-1}. HRMS (ES): m/z = 298.155 (calcd. 296.158 for $C_{10}H_{18}N_9O_2$, $[M]^+$).

4. Conclusions

In the growing field of *N*-heterocyclic carbene (NHC) catalysis, one of the most recent and exciting concepts is the thermally triggered release of the catalytically active species [27]. The new azole-substituted triazenes could become of interest as metal-free, labile NHC progenitors capable of switching on latent reactions. More research is needed with regard to solvent and temperature applied in order to liberate an active NHC.

Acknowledgments: The authors are grateful to Ulrich J. Griesser and Elisabeth Gstrein for the generous measurements of DSC and TGA.

Author Contributions: Simone Haslinger carried out experimental work (synthesis, crystallization and characterization), and Gerhard Laus and Herwig Schottenberger conceived and designed this study. Gerhard Laus wrote the manuscript. Volker Kahlenberg and Klaus Wurst determined the crystal structures. Thomas Bechtold contributed the cyclic voltammetry measurements. Stefan Vergeiner recorded the mass spectra.

Conflicts of Interest: The authors declare no conflict of interest.

References

1. Laus, G.; Schwärzler, A.; Schuster, P.; Bentivoglio, G.; Hummel, M.; Wurst, K.; Kahlenberg, V.; Lörting, T.; Schütz, J.; Peringer, P.; *et al. N,N′*-Di(alkyloxy)imidazolium Salts: New Patent-free Ionic Liquids and NHC Precatalysts. *Z. Naturforsch.* **2007**, *62b*, 295–308. [CrossRef]
2. Kitamura, M.; Kato, S.; Yano, M.; Tashiro, N.; Shiratake, Y.; Sando, M.; Okauchi, T. A reagent for safe and efficient diazo–transfer to primary amines: 2–azido–1,3–dimethylimidazolinium hexafluorophosphate. *Org. Biomol. Chem.* **2014**, *12*, 4397–4406. [CrossRef] [PubMed]
3. Zanirato, P.; Cerini, S. On the utility of the azido transfer protocol: Synthesis of 2- and 5-azido *N*-methylimidazoles, 1,3-thiazoles and *N*-methylpyrazole and their conversion to triazole–azole bisheteroaryls. *Org. Biomol. Chem.* **2005**, *3*, 1508–1513. [CrossRef] [PubMed]
4. Khramov, D.M.; Bielawski, C.W. Triazene formation via reaction of imidazol-2-ylidenes with azides. *Chem. Commun.* **2005**, *39*, 4958–4960. [CrossRef] [PubMed]
5. Khramov, D.M.; Bielawski, C.W. Donor–Acceptor Triazenes: Synthesis, Characterization, and Study of Their Electronic and Thermal Properties. *J. Org. Chem.* **2007**, *72*, 9407–9417. [CrossRef] [PubMed]
6. Kunetskiy, R.A.; Cisarova, I.; Saman, D.; Lyapkalo, I.M. New Lipophilic 2-Amino-*N,N′*-dialkyl-4,5-dimethylimidazolium Cations: Synthesis, Structure, Properties, and Outstanding Thermal Stability in Alkaline Media. *Chem. Eur. J.* **2009**, *15*, 9477–9485. [CrossRef] [PubMed]
7. Tennyson, A.G.; Ono, R.J.; Hudnall, T.W.; Khramov, D.M.; Er, J.A.V.; Kamplain, J.W.; Lynch, V.M.; Sessler, J.L.; Bielawski, C.W. Quinobis(imidazolylidene): Synthesis and Study of an Electron-Configurable Bis(N-Heterocyclic Carbene) and Its Bimetallic Complexes. *Chem. Eur. J.* **2010**, *16*, 304–315. [CrossRef] [PubMed]
8. Ghadwal, R.S.; Roesky, H.W.; Granitzka, M.; Stalke, D. A Facile Route to Functionalized N–Heterocyclic Carbenes (NHCs) with NHC Base-Stabilized Dichlorosilylene. *J. Am. Chem. Soc.* **2010**, *132*, 10018–10020. [CrossRef] [PubMed]
9. Tennyson, A.G.; Moorhead, E.J.; Madison, B.L.; Er, J.A.V.; Lynch, V.M.; Bielawski, C.W. Methylation of Ylidene-Triazenes: Insight and Guidance for 1,3-Dipolar Cycloaddition Reactions. *Eur. J. Org. Chem.* **2010**, *2010*, 6277–6282. [CrossRef]
10. Patil, S.; Bugarin, A. Crystal structure of (*E*)-1,3-dimethyl-2-[3-(3-nitrophenyl)triaz-2-en-1-ylidene]-2,3-dihydro-1*H*-imidazole. *Acta Crystallogr.* **2014**, *E70*, 224–227. [CrossRef] [PubMed]
11. Lysenko, S.; Daniliuc, C.G.; Jones, P.G.; Tamm, M. Tungsten alkylidyne complexes with ancillary imidazolin-2-iminato and imidazolidin-2-iminato ligands and their use in catalytic alkyne metathesis. *J. Organomet. Chem.* **2013**, *744*, 7–14. [CrossRef]

12. Naef, R.; Balli, H. Synthesis, Structure and Photochemical Properties of 4,4′,7,7′-Tetra-substituted1,1′,3,3′-Tetraethylbenzimidazolotriazatrimethine Cyanines. *Helv. Chim. Acta* **1978**, *61*, 2958–2973. [CrossRef]
13. Hanot, V.P.; Robert, T.D.; Kolnaar, J.J.A.; Haasnoot, J.G.; Kooijman, H.; Spek, A.L. Crystal structure and magnetic properties of a μ-halogeno-bridged copper(II) chain with neutral planar [Cu(batt)Cl] units (Hbatt = 1,3-bis[3-(5-amino-1,2,4-triazolyl)]triazene). *Inorg. Chim. Acta* **1997**, *256*, 327–329. [CrossRef]
14. Hanot, V.P.; Robert, T.D.; Haasnoot, J.G.; Kooijman, H.; Spek, A.L. Crystal structure and resonance Raman spectroscopic study of {1,3-bis[3-(5-amino-1,2,4-triazolyl)]triazenido-N′4,N2,N″4}chloro palladium(II)-methanol (1/1). *J. Chem. Cryst.* **1998**, *28*, 343–351. [CrossRef]
15. Hanot, V.P.; Robert, T.D.; Haasnoot, J.G.; Kooijman, H.; Spek, A.L. Crystal structure and spectroscopic study of bis{1,3-bis[3-(5-amino-1,2,4-triazolyl)]triazenido-N′4,N2,N″4}nickel(II) tetrahydrate. *J. Chem. Cryst.* **1999**, *29*, 299–308. [CrossRef]
16. Serebryanskaya, T.V.; Ivashkevich, L.S.; Lyakhov, A.S.; Gaponik, P.N.; Ivashkevich, O.A. 1,3-Bis(2-alkyltetrazol-5-yl)triazenes and their Fe(II), Co(II) and Ni(II) complexes: Synthesis, spectroscopy, and thermal properties. Crystal structure of Fe(II) and Co(II) 1,3-bis(2-methyltetrazol-5-yl)triazenide complexes. *Polyhedron* **2010**, *29*, 2844–2850. [CrossRef]
17. Eulgem, P.J.; Klein, A.; Maggiarosa, N.; Naumann, D.; Pohl, R.W.H. New Rare Earth Metal Complexes with Nitrogen-Rich Ligands: 5,5′-Bitetrazolate and 1,3-Bis(tetrazol-5-yl)triazenate–On the Borderline between Coordination and the Formation of Salt-Like Compounds. *Chem. Eur. J.* **2008**, *14*, 3727–3736. [CrossRef] [PubMed]
18. Chopra, D.; Guru Row, T.N. Role of organic fluorine in crystal engineering. *CrystEngComm* **2011**, *13*, 2175–2186. [CrossRef]
19. D'Oria, E.; Novoa, J.J. On the hydrogen bond nature of the C–H···F interactions in molecular crystals. An exhaustive investigation combining a crystallographic database search and ab initio theoretical calculations. *CrystEngComm* **2008**, *10*, 423–436. [CrossRef]
20. Allen, F.H.; Kennard, O.; Watson, D.G.; Brammer, L.; Orpen, A.G.; Taylor, R. Tables of Bond Lengths determined by X-Ray and Neutron Diffraction. Part I. Bond Lengths in Organic Compounds. *J. Chem. Soc. Perkin Trans.* **1987**, *2*, S1–S19. [CrossRef]
21. Kamlet, M.J.; Abboud, J.-L.M.; Taft, R.W. The Solvatochromic Comparison Method. The π* Scale of Solvent Polarities. *J. Am. Chem. Soc.* **1977**, *99*, 6027–6038. [CrossRef]
22. Taft, R.W.; Kamlet, M.J. The Solvatochromic Comparison Method. The α Scale of Solvent Hydrogen-Bond Donor (HBD) Acidities. *J. Am. Chem. Soc.* **1976**, *98*, 2886–2894. [CrossRef]
23. Kamlet, M.J.; Taft, R.W. The Solvatochromic Comparison Method. The β Scale of Solvent Hydrogen-Bond Acceptor (HBA) Basicities. *J. Am. Chem. Soc.* **1976**, *98*, 377–383. [CrossRef]
24. Marcus, Y. The Properties of Organic Liquids that are Relevant to their Use as Solvating Solvents. *Chem. Soc. Rev.* **1993**, *22*, 409–416. [CrossRef]
25. Holbrey, J.D.; Reichert, W.M.; Swatloski, R.P.; Broker, G.A.; Pitner, W.R.; Seddon, K.R.; Rogers, R.D. Efficient, halide free synthesis of new, low cost ionic liquids: 1,3-dialkylimidazolium salts containing methyl- and ethyl-sulfate anions. *Green Chem.* **2002**, *4*, 407–413. [CrossRef]
26. Schwärzler, A.; Laus, G.; Kahlenberg, V.; Wurst, K.; Gelbrich, T.; Kreutz, C.; Kopacka, H.; Bonn, G.; Schottenberger, H. Quaternary 4-amino-1,2,4-triazolium Salts: Crystal structures of Ionic Liquids and *N*-heterocyclic carbene (NHC) complexes. *Z. Naturforsch.* **2009**, *64b*, 603–616. [CrossRef]
27. Naumann, S.; Buchmeiser, M.R. Liberation of N-heterocyclic carbenes (NHCs) from thermally labile progenitors: Protected NHCs as versatile tools in organo- and polymerization catalysis. *Catal. Sci. Technol.* **2014**, *4*, 2466–2479. [CrossRef]